

## In-building power lines as high-speed communication channels: channel characterization and a test channel ensemble

Tooraj Esmailian<sup>1,\*†</sup>, Frank R. Kschischang<sup>2</sup> and P. Glenn Gulak<sup>2</sup>

<sup>1</sup>*Cogency Semiconductor Inc., 362 Terry Fox Drive, Kanata, Ont., Canada K2K 2P5*

<sup>2</sup>*The Edward S. Rogers Sr. Department of Electrical and Computer Engineering, University of Toronto,  
Toronto, Ont., Canada M5S 3G4*

### SUMMARY

In-building power lines have often been considered as attractive media for high-speed data transmission, particularly for applications like home networking. In this paper, we develop models for power line channels based both on theoretical considerations and practical measurements. We consider power line channel frequency response and noise models in the 1–30 MHz band and propose a number of power line test channels in which to measure the performance of power line modems. Copyright © 2003 John Wiley & Sons, Ltd.

KEY WORDS: power line communication; channel characteristics; channel capacity; channel simulator

### 1. INTRODUCTION

For many years, power lines have been used for low speed (< 30 kbps) data communication in applications like power distribution automation and remote metre reading [1, 2], and local area networks [3–10]. Today, due to the increasing importance of networking in homes, offices and industrial buildings, power lines are being considered as a candidate medium also for high speed (> 2 Mbps) data transmission [11, 12].

The key advantage of power lines is that they provide a ‘pre-installed’ infrastructure of wires and wall outlets that are easy to access throughout a building. On the other hand there are many challenges in using this medium for high-speed communication; all originate from the fact that this medium was designed for distribution of electrical power, not for communication.

To understand the challenges of power line communication, and to design suitable high-speed data transmission equipment, one must have a good understanding of the communication channel characteristics; in particular, the range of channel frequency response, and the characteristics of the channel noise. These characteristics can be quite diverse among different buildings because of different wiring structures, different wire types, and different appliances

---

\*Correspondence to: T. Esmailian, Cogency Semiconductor Inc., 362 Terry Fox Drive, Kanata, Ontario K2K 2P5, Canada.

†E-mail: tooraj@cogency.com

connected to the electric circuit. For performance characterization of power line modems, it would be useful to have a number of test channels, each representative of a class of power line channels. Ideally the union of these classes would cover a large percentage of buildings in which the use of power line modems is probable.

In this paper, we describe the methodology that we have followed to develop a number of test channels. In Section 2, we introduce the general structure of power circuits in residential buildings as specified by the US national electric code (NEC) [13]. In Section 3, using the theory of transmission lines, we calculate the channel transfer function for a sample channel based on actual power cable parameters. We also provide the results of experimental measurements of the channel transfer function and compare them with theoretical predictions. In Section 4, we describe the results of our experimental measurements of background and impulsive noise and we propose some representative noise models. Based on the results of Section 3, we propose a number of NEC-compliant power line test channels in Section 5. We also provide the distribution of channel capacity as well as the distribution of RMS delay spread for these power line channels.

## 2. POWER DISTRIBUTION CIRCUITS

In this section, we describe the general structure of power line circuits in residential and commercial/industrial buildings. In Sections 4 and 5, we will use this general structure in combination with the NEC rules to develop a statistical model for in-building power line channels and choose a number of test channels.

### 2.1. Power distribution

Electrical energy is usually distributed in a high-voltage form, and then down converted in several stages using transformers before delivery to the consumer. Figure 1 shows the final distribution transformer in typical power distribution circuits for residential and commercial/industrial buildings.

At high frequencies, the existence of the final distribution transformer prevents the effect of loads connected to one side of the transformer from being observed at the other side. This isolation at high frequencies is due to the fact that the input impedance of the transformer windings is virtually infinite. The secondary windings can therefore be modelled as an open circuit, and the secondary windings of the final distribution transformer can be considered as the starting point of any in-building power line communication channel.

In typical configurations, there are usually several residences (typically between 5 and 20, in U.S.A. and Canada [15]) connected to the secondary side of the same transformer. This implies that communication signals from one residence can pass to another. This leakage can be prevented by suitable signal filtering, or, alternatively, one may permit the passage of communication signals between residences, and maintain security via some suitable encryption scheme. (The HomePlug<sup>‡</sup> standard, e.g. specifies the use of DES [16].) We will not be concerned with issues of secure communication in this paper.

<sup>‡</sup>The HomePlug Power Line Alliance is a nonprofit industry association established to provide a forum for the creation of an open specification for home power line networking products and services.

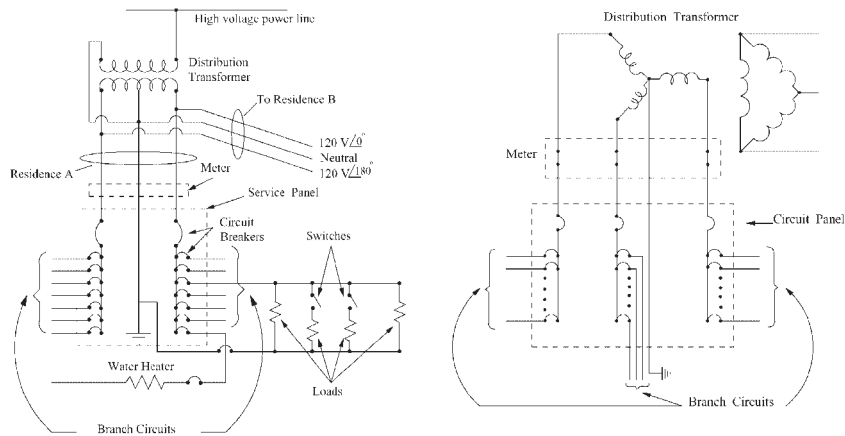


Figure 1. *Left*: Residential power distribution circuit (based on [14]). *Right*: Commercial/Industrial power distribution circuit (based on [14]).

The secondary side of the transformer is usually connected to the building panel board using three (or four) wires: one wire for neutral and the others for different voltage phases. From the panel board, power is then distributed using several branch circuits throughout the building, and these branch circuits can be used as communications media for suitably designed modems attached to different electrical outlets.

As can be seen from Figure 1, it is possible that communication may need to take place between modems connected to different phases. In such a situation, the communication signal will undergo some loss. Fortunately, this loss is small at high frequencies, e.g. frequencies larger than 1 MHz [17], since all phases are located in a close proximity at the panel board and therefore there is a large cross-talk between the phases due to capacitive coupling. Thus, throughout this paper, we will assume that any signal degradation caused by inter-phase communication is negligible.

## 2.2. Communication via branch circuits

For the purposes of this work, we simplify the branch circuit structure to that shown in Figure 2. For simplicity, the multiple service wires have been represented by a single thick line, and the multiple branch wires have been represented by thinner lines. On each branch there are a number of black hexagons representing electrical outlets. In a North American home there are on average 44 such outlets [18]. Of course a complete power circuit also contains a number of loads connected to the outlets, usually via some connecting cords; these are not shown in Figure 2.

In the absence of noise, we will model the channel between any pair of outlets as a linear time-invariant system, characterized by some transfer function. In this relatively complicated network, there are many parameters that have considerable effect on the channel transfer function. These include: the number of branch circuits, the size and length of branch circuits, the number of outlets on each branch circuit, the distance between neighbouring outlets on the same branch, the impedance of loads connected to the outlets, the size and length of cords that connect loads to the outlets, and the size and length of the service wires themselves.

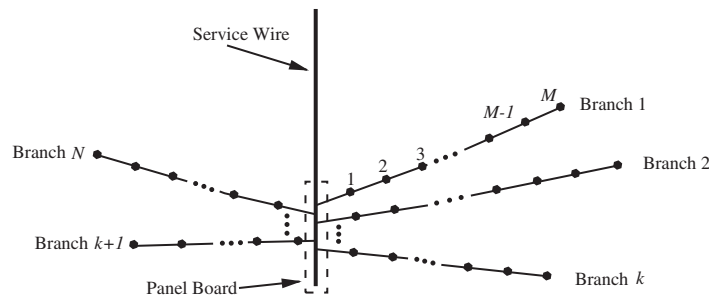


Figure 2. A simplified diagram of residential power line circuits. Each line represents two physical lines (a phase and a neutral). Each black hexagon represents an electrical outlet.

Fortunately, the building size, electric power requirements, and the NEC place limits on the values of many of these parameters. In the next section, we will study some of the more important limits, which will be used in Section 5 to develop an ensemble of channel models. To model the impedance of loads connected to the power circuit we use the results of Reference [17].

### 2.3. Limits on the power line circuit parameters

*Wire gauge:* One of the parameters in a power line circuit is the size of branch circuit wires (wire gauge). In general, the current and voltage drop requirements of electrical equipment connected to outlets, and the distance of the branch circuit outlets to the panel board determine the minimum possible size of branch circuit wires. The most common wire sizes in residential buildings are No. 14, 12 and 10 AWG [19]. Our later results show that the channel transfer function is relatively insensitive to the wire gauge.

*Number of outlets per branch:* According to the NEC, the total load on a typical branch circuit must not exceed 80% of the circuit current-carrying capacity when the load is continuous, i.e. for a load in continuous operation for 3 h or longer [13]. In residential applications, most designers allow 300 W per duplex receptacle (2.5 A at 120 V) unless it is provided for a known usage [20]. At 120 V, this implies a maximum of four to five outlets per 15 A circuit, six to seven per 20 A circuit, and nine to ten per 30 A circuit, assuming each outlet consumes 2.5 A, and the 80% limit is maintained.

*Number of branch circuits:* Our studies of the required number of branch circuits for a building (not including special branches for heavy loads like an electric range) indicate that the required total electrical power requirements scale with the building floor area, roughly at the rate of 140 W per square metre (1.2 A for a 120 V circuit).

*Maximum branch circuit length:* This parameter depends on the building size and architectural plan. Since wiring is usually constrained to run in walls, it is reasonable to assume that the maximum branch length is equal to the half of the building perimeter<sup>§</sup> plus the required height of the wire for going from the panel board to the furthest floor. We consider an extra 10% for the possible extra wires required for possible obstructions in the walls.

<sup>§</sup>For the worst case in which the panel board is located exactly at one of the corners of the building.

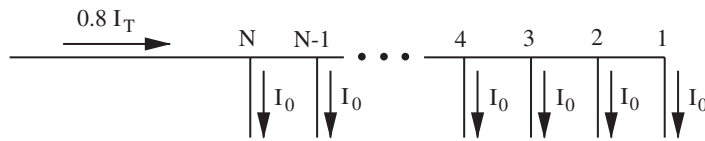


Figure 3. A simplified diagram of a sample branch circuit.  $I_T$  is the breaker current,  $I_0$  is the maximum current of each outlet, and  $N$  is the number of outlets connected to the branch circuit.

*Voltage drop limits.* Another limit that the NEC places on the branch length and size is based on the wire voltage drop. The NEC specifies that all branch wires should be sized so that the voltage drop never exceeds 3%. The voltage drop,  $V_d$ , in any two-wire circuit consisting of mostly resistance type loads with negligible inductance may be calculated as

$$V_d = 2kLI/A \tag{1}$$

where,  $k$  is the resistivity of conductor metal,  $L$  is the length of conductor,  $I$  is the conductor current, and  $A$  is the area of conductor. For example, the maximum length of a No. 12 AWG copper wire carrying 10 A current is approximately 33 m.

Usually outlets are more concentrated toward the end of branch circuits rather than the beginning of branch circuits (which are connected to the panel board). The worst case in terms of voltage drop is when outlets are located at the minimum possible distance next to each other,  $l_{min}$ . In this case, the maximum possible length for a branch circuit,  $L_{max}$ , when the circuit breaker has a current capacity of  $I_T$ , can be approximately calculated as

$$L_{max} = (N - 1)l_{min} + \frac{AV_d + kl_{min}(N - 1)(NI_0 - 1.6I_T)}{1.6kI_T} \tag{2}$$

in which  $N$  represents the number of outlets on the branch circuit, see Figure 3.

*Maximum inter-outlet spacing:* Another parameter that is limited by the NEC rules is the maximum distance between two neighbour outlets on the same branch circuit. ‘Article 210-52’ of the NEC requires that no point on any floor of a typical room be farther than approximately 1.8 m from any electrical outlet [20]. Therefore, we can simply assume that the maximum possible distance between two neighbouring outlets on a branch circuit is 3.6 m for residential buildings.

### 3. POWER LINE CABLE TRANSFER FUNCTION

A typical power line cable consists of three conductors: one connected to a phase, one connected to the neutral, and the other connected to ground. Each of the phase and neutral conductors is covered by an insulator and the set of three conductors is placed inside another insulator. Two of these three conductors suffice to create a communication channel. Since the phase and neutral conductors have equal wire gauge (usually larger than that of the ground conductor) we use these two conductors as the communication channel, although it is possible to use other combinations of conductors<sup>¶</sup>.

<sup>¶</sup>Because of the proximity of all three wires in a branch circuit (phase, neutral and ground) there is a large coupling between them. However, it might be possible to perform a co-ordinated transmission between these wires, e.g. phase and ground as one channel and neutral and ground as another channel.

We study channel transfer functions using *chain matrix* (ABCD matrix) theory [21], which we use to compute the transfer function of some sample power line channels, and study the effect of channel parameters such as wire size, bridge-tap length, and location of bridge taps. We compare these theoretical results with some experimental measurements.

### 3.1. Modelling

In this section, we will assume that the exact structure and type of wires as well as loads that are connected to the channel are known perfectly.

*3.1.1. ABCD matrix and channel transfer function.* The ABCD representation for a two-port circuit is very convenient for the calculation of channel transfer functions [22]. In Figure 4, the relation between  $V_1$ ,  $I_1$ ,  $V_2$  and  $I_2$  (the input voltage and current and output voltage and current of a two port network) can in general be represented as

$$\begin{bmatrix} V_1 \\ I_1 \end{bmatrix} = \begin{bmatrix} A & B \\ C & D \end{bmatrix} \begin{bmatrix} V_2 \\ I_2 \end{bmatrix} \quad (3)$$

where  $A$ ,  $B$ ,  $C$  and  $D$  are appropriately chosen constants. It is easy to show that if we have a cascade of two-port circuits, the ABCD representation of this circuit is the product of the ABCD matrices for the individual two-port circuits.

Now consider the circuit of Figure 4, in which all voltages and currents are presented by their phasors. Using the ABCD model for the two-port box in this figure it is easy to calculate the transfer function of the circuit ( $V_L/V_s$ ) as

$$H = \frac{V_L}{V_s} = \frac{Z_L}{AZ_L + B + CZ_L Z_s + DZ_s} \quad (4)$$

Also it is easy to calculate input impedance of the two-port circuit ( $Z_1$ ) as

$$Z_1 = \frac{V_1}{I_1} = \frac{AZ_L + B}{CZ_L + D} \quad (5)$$

Two parallel cables (for example power line phase and neutral cables) can be modelled as a transmission line. A transmission line can be characterized by its *characteristic impedance*  $Z_c$ ,

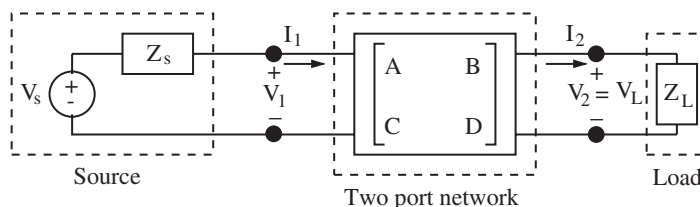


Figure 4. A two port network connected to a voltage source and a load.

and its *propagation constant*  $\gamma$  [23]. By measuring the per-unit-length parameters of a cable it is easy to calculate the characteristic impedance  $Z_c$ , and propagation constant  $\gamma$  of the cable as

$$Z_c = \sqrt{\frac{R + j\omega L}{G + j\omega C}} \tag{6}$$

$$\gamma = \sqrt{(R + j\omega L)(G + j\omega C)} \tag{7}$$

where  $R, L, G$  and  $C$  are per-unit-length resistance ( $\Omega/m$ ), inductance ( $H/m$ ), conductance ( $S/m$ ) and capacitance ( $F/m$ ), respectively, and  $\omega$  is frequency ( $rad/s$ ). The ABCD matrix for a transmission line with characteristic impedance of  $Z_c$  and propagation constant of  $\gamma$  and a length of  $l$  can be calculated as

$$\begin{bmatrix} A & B \\ C & D \end{bmatrix} = \begin{bmatrix} \cosh(\gamma l) & Z_c \sinh(\gamma l) \\ \frac{1}{Z_c} \sinh(\gamma l) & \cosh(\gamma l) \end{bmatrix} \tag{8}$$

*3.1.2. Transfer function of a transmission line with bridge tap.* The transfer function of the two-port circuit of Figure 4 is given by (4), and the ABCD parameters of a transmission line can be computed using (8). Therefore, the calculation of the transfer function for a simple transmission line is straightforward. Consider, for example, Figure 5(a), which shows a transmission line with one bridge tap.

If we replace the bridge tap with the equivalent impedance ( $Z_{eq}$ ), which can be seen from terminals  $A$  and  $B$ , the circuit can be simplified to that of Figure 5(b). In this figure,  $Z_{eq}$  can be calculated as

$$Z_{eq} = Z_c \frac{Z_{br} + Z_c \tanh(\gamma_{br} d_{br})}{Z_c + Z_{br} \tanh(\gamma_{br} d_{br})} \tag{9}$$

where  $Z_c$  and  $\gamma_{br}$  are characteristic impedance and propagation constant of the branch circuit.

In Figure 5(b) the circuit has been partitioned into four cascade two-port sub-circuits. For each sub-circuit it is possible to calculate an ABCD matrix ( $\Phi_i, i = 0, 1, 2, 3$ ) and the ABCD matrix for the total circuit ( $\Phi$ ) is  $\Phi = \prod_{i=0}^3 \Phi_i$ , where

$$\Phi_0 = \begin{bmatrix} 1 & Z_s \\ 0 & 1 \end{bmatrix}, \quad \Phi_1 = \begin{bmatrix} \cosh(\gamma_1 d_1) & Z_1 \sinh(\gamma_1 d_1) \\ \frac{1}{Z_1} \sinh(\gamma_1 d_1) & \cosh(\gamma_1 d_1) \end{bmatrix}, \quad \Phi_2 = \begin{bmatrix} 1 & 0 \\ \frac{1}{Z_{eq}} & 1 \end{bmatrix}$$

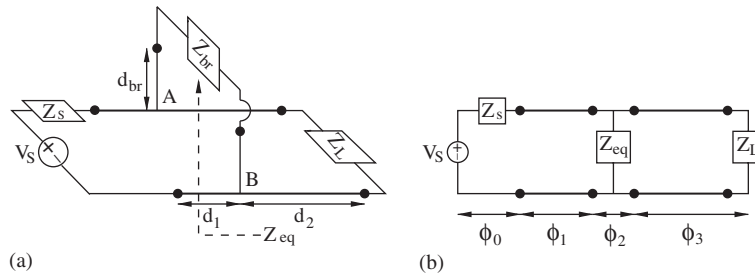


Figure 5. (a) A transmission line with one bridge tap connection, (b) equivalent of the left-hand circuit.

and

$$\Phi_3 = \begin{bmatrix} \cosh(\gamma_2 d_2) & Z_2 \sinh(\gamma_2 d_2) \\ \frac{1}{Z_2} \sinh(\gamma_2 d_2) & \cosh(\gamma_2 d_2) \end{bmatrix}$$

where  $Z_1$ ,  $\gamma_1$ ,  $Z_2$  and  $\gamma_2$  are the characteristic impedances and propagation constants for the second and fourth sub-circuits of Figure 5(b). Using the above equations the ABCD matrix elements for the circuit of Figure 5 are given by

$$\begin{aligned} A &= \cosh(\gamma_2 d_2) \alpha + \frac{\sinh(\gamma_2 d_2)}{Z_2} \beta \\ B &= Z_2 \cosh(\gamma_2 d_2) \alpha + \cosh(\gamma_2 d_2) \beta \\ C &= \cosh(\gamma_2 d_2) \xi + \frac{\sinh(\gamma_2 d_2)}{Z_2} \vartheta \\ D &= Z_1 \sinh(\gamma_1 d_1) \xi + \cosh(\gamma_2 d_2) \vartheta \end{aligned}$$

where

$$\begin{aligned} \alpha &= \cosh(\gamma_1 d_1) + \frac{Z_s}{Z_1} \sinh(\gamma_1 d_1) \\ \beta &= Z_1 \sinh(\gamma_1 d_1) + Z_s \cosh(\gamma_1 d_1) \\ \xi &= [Z_1 \cosh(\gamma_1 d_1) + Z_s \sinh(\gamma_1 d_1) + Z_{\text{eq}} \sinh(\gamma_1 d_1)] / (Z_1 Z_{\text{eq}}) \\ \vartheta &= [Z_1 \sinh(\gamma_1 d_1) + Z_s \cosh(\gamma_1 d_1)] / Z_{\text{eq}} + \cosh(\gamma_1 d_1) \end{aligned}$$

Then, by using (4), the circuit transfer function can be calculated easily. For channels with more bridge taps, the calculation of the channel transfer function based on this method is straightforward, but the formula is more complex.

### 3.2. Analytical results

To explore the range of possible power line channels, we now present the results of our analysis applied to a variety of wire configurations. As an example we have used a channel with four bridge taps, as shown in Figure 6. In this figure,  $d_1, \dots, d_5$  are the lengths of different channel sections, and  $l_1, \dots, l_4$  are the lengths of bridge taps.

By changing various channel parameters (e.g. the channel length, bridge-tap length, and wire size) a variety of channels are obtained. We define the channel length as the distance between transmitter and receiver, which, in the case of Figure 6(a), is  $\sum_{i=1}^5 d_i$ . In a similar way the total bridge tap length for Figure 6(a) is defined as  $\sum_{i=1}^4 l_i$ .

Figure 6(b) shows the effect of channel length on attenuation. In this analysis we have used the realistic assumption that by increasing the channel length, it is very likely that the number of bridge taps and total bridge tap length increase. Based on this assumption, by increasing the channel length, attenuation increases.

Further analysis shows that the location and length of bridge-taps as well as impedance of loads connected to the bridge-taps have considerable effect on the channel transfer function [24]. We note also that loads in excess of approximately 1 k $\Omega$  can be virtually considered as an open

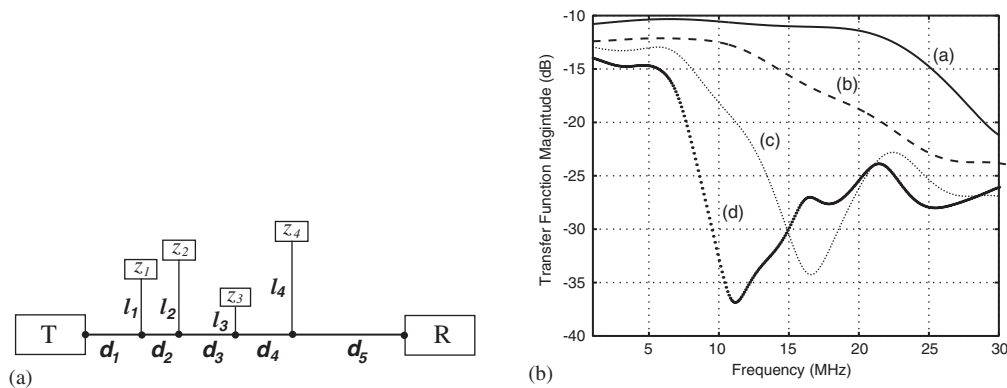


Figure 6. (a) A sample power line channel, (b) attenuation of the sample channel with different channel and bridge tap lengths. Here  $L_c$ ,  $L_b$  and  $N$  represent the channel length, total bridge tap length and number of bridge taps in the channel. (a) (6 m, 2 m, 1), (b) (10 m, 4 m, 2), (c) (15 m, 6 m, 3), (d) (25 m, 10 m, 4). All wires are 14 AWG and loads are:  $Z_1 = 50 + j100 \Omega$ ,  $Z_2 = 150 \Omega$ ,  $Z_3 = 20 - j100 \Omega$ , and  $Z_4 = 250 \Omega$ .

circuit. We also observe that there is not a significant difference between the channel attenuation of 12 and 14 AWG wires, which are the most common wire sizes in residential buildings.

### 3.3. Measurement results

We have made frequency response measurements for in-building power line channels in the frequency range of 1–15 MHz [25]. The measurement set-up is shown in Figure 7(a). The transmitter consists of a sinusoidal signal generator connected to a high-pass filter consisting of two  $1\mu\text{F}$  capacitors and a wide-band RF transformer<sup>||</sup> (for blocking the 60 Hz, 110 V power line voltage). The receiver consists of a high-pass filter and a digital oscilloscope. In this figure  $Z_I$  represents the receiver input impedance.

Measurements have been performed between phase and ground (P–G), neutral and ground (N–G), and phase and neutral (P–N) wires in the power circuit and some of the results are shown in Figure 8. As can be seen, the frequency response exhibits considerable frequency-dependent variation, due to the specific wiring configurations encountered. The frequency-dependent channel fading is the result of reflections and multipath propagation. One main source for reflection and multipath propagation is impedance discontinuity. At impedance discontinuities part of the transmitted signal is reflected. The reflected signals can be received by the receiver and the addition of the reflected signal and original signal can be constructive or destructive, in which case signal fading may be generated. There are many possible reasons for impedance discontinuity, such as change of gauge of wires connected to each other, connected loads or branch wires, etc.

On the whole, the channels exhibit behaviour that is similar to analytical predictions. Since the exact structure of the circuit in which we have made our measurements was unknown, it was not possible to find channel attenuation based on theory and compare it with our measurements. However, by comparing analytical results and measurements we see that they share common properties. First, both measurement and theory show that attenuation increases

<sup>||</sup>This transformer has a flat frequency response in the frequency range of 30 kHz up to 50 MHz.

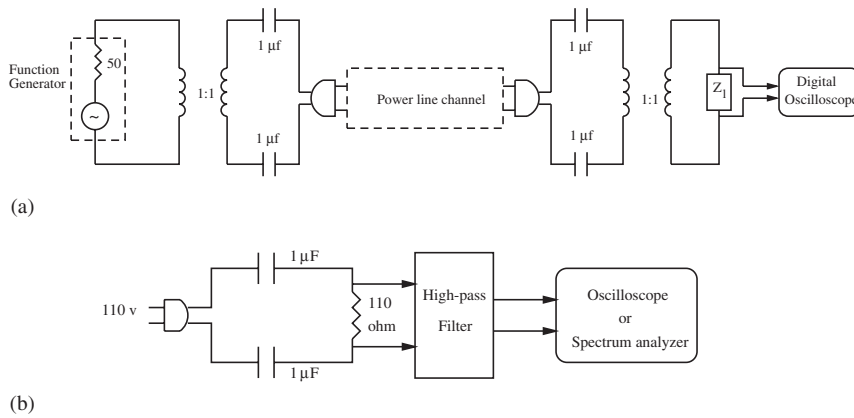


Figure 7. (a) Channel frequency response measurement set-up, (b) noise measurement set-up.

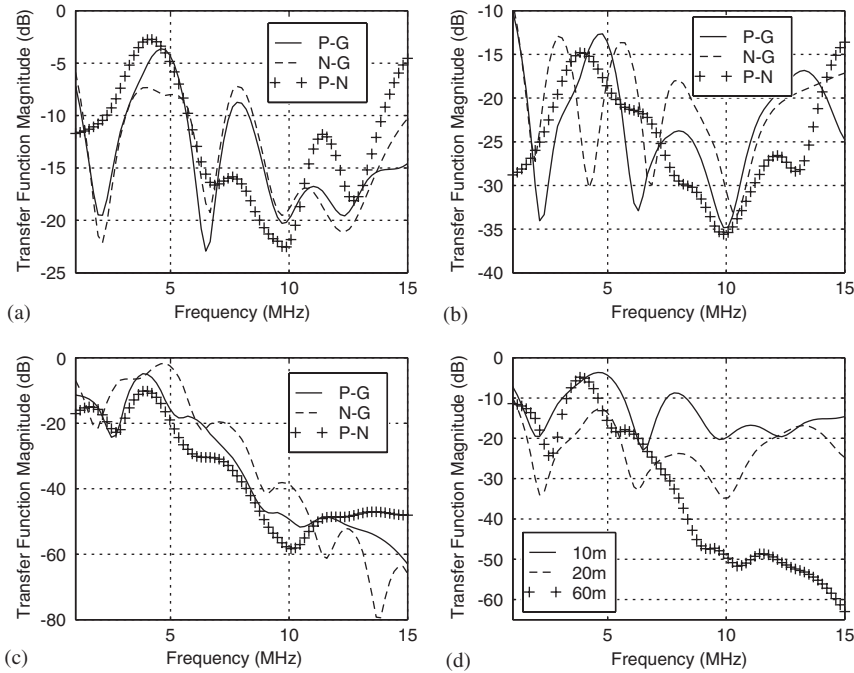


Figure 8. Experimental measurements of frequency response magnitude for different cable lengths. (a) 10 m, (b) 20 m, (c) 60 m and (d) P-G (phase to ground) for 10 m, 20 m and 60 m cables. Note that in these measurements the channels may include bridge taps.

as a function of frequency. Both measurement and theory show channel attenuation varying from around 10–60 dB (or more). Second, both measurement and theory show that the channel exhibits frequency selective attenuation. Third, unsurprisingly both measurement and theory show that increasing the channel length is very likely to cause increased attenuation.

## 4. NOISE

In this section, results of our measurements on the power line channels background and impulsive noise are presented. Based on these results we propose some models for pseudorandom generation of noise samples, which are useful for simulation of a power line modem.

### 4.1. Background noise

Usually background noise in a communications system limits the channel capacity. We measured the background noise for in-building power line channels [25] using the measurement setup shown in Figure 7(b).

A digital oscilloscope\*\* was used to measure the noise in the time domain, and a spectrum analyser†† was used for measuring the noise spectrum. Two 1  $\mu$ F capacitors were used to block the power signal, and a seventh-order, 0.25 dB, high-pass Chebyshev filter was used to block all other components under 1 MHz.

*4.1.1. Frequency domain.* Figure 9 (left side) shows one example of the measured background noise PSD and its corresponding mathematical approximation. Although there is considerable variation, the macroscopic noise PSD is captured by a simple three-parameter model

$$S_n(f) = a + b|f|^c \text{ dBm/Hz} \quad (10)$$

where  $a$ ,  $b$  and  $c$  are parameters depending on the location of measurement, and  $f$  is the frequency in MHz. In the best case among our measurements  $(a, b, c) = (-140, 38.75, -0.720)$  and for the worst case  $(a, b, c) = (-145, 53.23, -0.337)$ . A similar model is proposed in Reference [26].

*4.1.2. Time domain.* Figure 9 (right hand) shows the calculated noise PDF compared with a Gaussian distribution with the same variance. Although the background noise distribution looks Gaussian near the mean, because of the heavy tails of the background noise distribution compared to a Gaussian distribution (as can be seen in Figure 9(b)), the result of a chi-square test (see, e.g. [27]) shows that the background noise is unlikely to be Gaussian.

### 4.2. Impulsive noise

Impulsive noise is usually characterized as a random pulse waveform whose amplitude is much higher than the background noise. Often, external devices connected to the power line are major sources of impulsive noise. Electric motors, silicon-controlled rectifiers (SCRs), and switching devices are some of the common impulsive noise generators. Among these devices, it is obvious that those that operate for a long period of time (for example SCRs in light dimmers) are more disruptive of data transfers over power lines.

Three important properties of impulsive noise are: amplitude, width and inter-arrival time distributions. These properties have been studied in [28], but in a low-frequency range (under

\*\* A Tektronix TDS 220 digital oscilloscope with a maximum sampling rate of 1 G samples/s was used.

†† An HP 8595E spectrum analyser with the maximum sensitivity of  $-110$  dBm for the resolution bandwidth of 300 Hz which is translated to a maximum sensitivity of  $-134$  dBm/Hz was used.

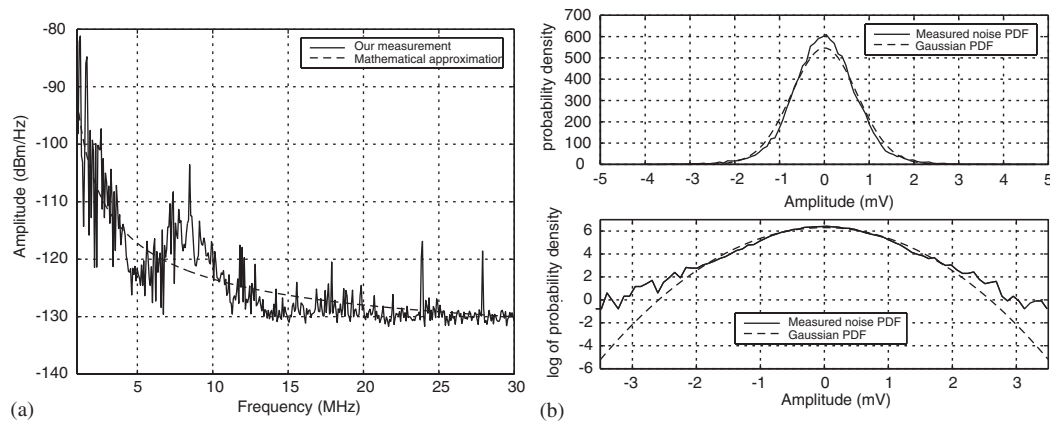


Figure 9. (Left): A sample of background noise power spectral density in a university building and mathematical approximation, (Right): (a) PDF of the measured background noise (with a variance of  $730 \mu\text{V}$ ) compared with a Gaussian distribution with the same variance, (b) log of PDFs of sub-plot (a).

450 kHz). We have presented the above-mentioned properties for impulsive noise, generated by an electric drill, and a light dimmer in Reference [25].

In impulsive noise measurements, we have classified a voltage sample of amplitude  $V$  as impulsive noise only when  $V$  exceeds a threshold  $T$  chosen so that background noise is unlikely to cross the threshold,  $T$ . The probability that a given recorded impulse's amplitude,  $V$ , exceeds some value  $v$  is:  $\Pr(V > v | V > T)$ .

Since SCRs are among the most disruptive sources of impulse noise, in the following sections we study properties of impulsive noise generated by SCRs.

Based on our measurements on amplitude, width, and inter-arrival time of impulsive noise generated by an SCR in a light dimmer we computed PDF of these three properties using the `hist()` function of MATLAB [29]. By looking at each PDF we chose a well-known distribution that looks like that PDF and then using least-squares curve fitting we found parameters of that distribution. The result is a simple approximation for the PDF.

**4.2.1. Amplitude distribution.** As an example the distribution of impulsive noise amplitude, generated by an SCR is measured. The amplitude of impulsive noise can be considered as a random variable  $\nu$  with a value  $v$  which our measurements show that it is in the range of  $8 \leq v \leq 17$  mV. Suppose that  $f(u)$  is a beta function with parameters  $a = 3$  and  $b = 2$  ( $f(u) = (\Gamma(5)/\Gamma(3))^2 u^2(1-u)$ ). A very simple model for the probability distribution function (PDF) of amplitude is as follows:

$$p_{\nu}(v) = f\left(\frac{v-8}{9}\right), \quad 8 \leq v \leq 17 \quad (11)$$

which is a beta-like distribution.

**4.2.2. Width distribution.** The distribution of width of impulsive noise generated by an SCR is calculated based on the noise samples. Again the width of impulsive noise can be considered as a

random variable  $\nu$  with a value of  $v$ . A very simple model for the PDF of width,  $p_\nu$ , is the following Gaussian mixture:

$$p_\nu(v) = P_1 \mathcal{N}(m_1, \sigma_1) + P_2 \mathcal{N}(m_2, \sigma_2) \quad (12)$$

where  $\mathcal{N}(m, \sigma) = (1/\sqrt{2\pi}\sigma) \exp(-(v-m)^2/2\sigma^2)$  and  $m_1 = 4.9$ ,  $\sigma_1 = 0.2$ ,  $m_2 = 4.2$ ,  $\sigma_2 = 0.25$ ,  $P_1 = 0.0763$ ,  $P_2 = 0.0318$  and  $v$  is in  $\mu\text{s}$ .

*4.2.3. Inter-arrival time distribution.* Again the inter-arrival time of impulsive noise can be considered as a random variable  $\nu$  with a value of  $v$ . A very simple model for the PDF of inter-arrival time,  $p_\nu$ , is as follows:

$$p_\nu(v) = \frac{1}{\Gamma(4.2)} v^{3.2} e^{-v} \quad (13)$$

which is a Gamma function with parameter  $n=4.2$ , and  $\nu$  is in ms.

## 5. SOME PROPOSED TEST CHANNELS

Based on the good agreement between analytical and measurement results given in the previous sections, we now develop a statistical model for power line channel transfer functions and provide some representative channel transfer functions as test channels.

As mentioned earlier, many power line circuit parameters, such as branch length and size, bridge-tap configuration, etc., depend on the type and size of the building. In this section, we consider only residential buildings. We divide residential buildings into three different types in terms of their size: small, medium and large. As representatives for small, medium and large size buildings we have considered buildings with a single-floor area of  $60 \text{ m}^2$  ( $645 \text{ ft}^2$ ),  $100 \text{ m}^2$  ( $1076 \text{ ft}^2$ ), and  $200 \text{ m}^2$  ( $2152 \text{ ft}^2$ ), respectively. The length and width of these three representative buildings are given in Table I.

If  $L$ ,  $W$ ,  $H$  and  $N$  represent the length, width, height of a floor, and the number of floors, respectively, the maximum possible branch length is around  $1.1(L+W+NH)$ . It has been assumed that the small and medium size representing buildings are single-floor, and the large representative building is two stories plus a basement. Also it has been assumed that the panel board is located at one of the corners of the building. (For the large building it is located in one corner of the basement.) A height of 3 m has been considered for each floor as well as basement. The maximum possible branch length for the three buildings is given in Table I. Since it is

Table I. Test channel specifications.

Building type	Single-floor area ( $\text{m}^2$ )	Branch size (AWG)	Current (A)	Max branch Length (m)	Number of Branches	Outlets per branch
Small	60 ( $6 \times 10$ )	14	15	17.5	6	5
Small	60 ( $6 \times 10$ )	12	20	17.5	5	7
Medium	100 ( $8 \times 12.5$ )	14	15	22.5	10	5
Medium	100 ( $8 \times 12.5$ )	12	20	22.5	8	7
Large	200 ( $12.5 \times 16$ )	12	20	38	15	7
Large	200 ( $12.5 \times 16$ )	10	30	38	10	10

possible that transmitter and receiver are located on two different branches, the maximum possible channel length is double the maximum branch length.

Using (2) and based on the maximum possible branch length which is being determined by the geometry of buildings, we have determined wire sizes and branch currents that can provide required power without violation of the NEC 3% voltage drop rule. These results as well as the number of required branch circuits and the number of outlets per branch circuit are shown in Table I. Although it may seem that the average outlets per building is more than 44, but it must be noted that the number of small buildings is much higher than medium or large buildings.

In developing our test channels, we have made the following assumptions. We assume that all branches in a building have the maximum possible number of outlets. We also assume size 18 AWG for the cords that connect different appliances to the outlets. We have assumed that 90% of such cords have a length uniformly distributed between 1 and 3 m, that 5% of them have a length uniformly distributed between 0 and 1 m, and the remaining 5% have a length uniformly distributed between 3 and 10 m. We have assumed a maximum of 3.6 m (NEC rule) and a minimum of 2 m for the inter-outlet spacing on any given branch.

Note that at low frequencies the impedance of appliances usually is much higher than the impedance of connecting cords, but at high frequencies the impedance of connecting cords is higher. It follows that the impedance of loads at low frequencies mainly determines the channel transfer function, while at higher frequencies, the impedance of connecting cords mainly determines the channel transfer function. For this reason we have used the distribution of impedance of loads in Reference [17] at 1 MHz in our analysis.

Based on the above assumptions, and using the channel model of Figure 2 we have developed a simulator program for the channel transfer function. Based on the building specifications we generate a pseudorandom power line circuit and compute the channel transfer function between a randomly chosen pair of outlets. We have used channel capacity to compare the different channels. For the capacity calculation we have used the water pouring method [30] and for the background noise PSD we have used the worst case among our measurements, as has been explained in Section 4. These capacity results assume additive Gaussian noise, which results in an under-estimation of the true channel capacity. The results of channel capacity distribution is explained in the next section.

### *5.1. Channel capacity distribution*

For each building and branch circuit size (specified in Table I) we have computed the channel capacity of 100 000 randomly generated channels, when the transmit power was 1 mW. Using this data we have computed the PDF of channel capacity and using it we have computed the cumulative density function (CDF) of capacity. We have chosen two points on the CDF curve. One is at the first percentile, where only 1% of channels have capacities less than the given capacity. The other one is at the 20th percentile. After finding the capacity at the first percentile, we have used our simulation program to find a channel that has a capacity very close to the capacity of the first percentile point. This channel can be used as one of our test channels. The same procedure has been performed for the 20th percentile point. The obtained channels are our test channels.

This process has been repeated for our six representative channels, which has provided us 12 test channel transfer functions. The result of our analysis for first medium size building has been presented in Figure 10.

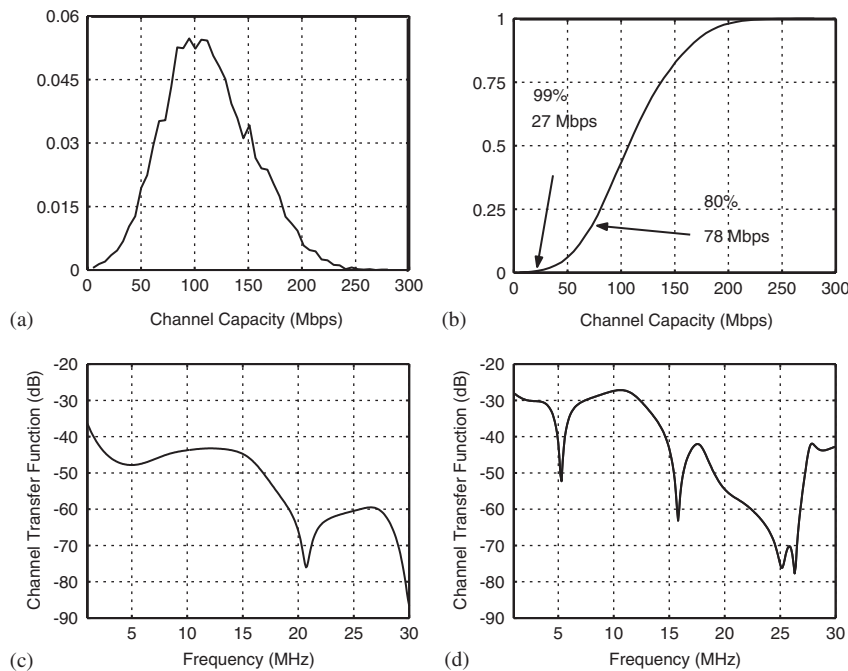


Figure 10. (a) PDF of capacity of medium size buildings with branch wires of size 14 AWG, (b) CDF of capacity, (c) a sample channel transfer function which has a capacity at the first percentile point, (d) a sample channel transfer function which has a capacity at the 20th percentile point. The transmit power is 1 mW.

Table II shows polynomial coefficients,  $a_n$ , that have been used to approximate these 12 test channels transfer function. If  $|H(f)|$  represents the magnitude of a channel transfer function we have

$$20 \log_{10}|H(f)| = \sum_{n=0}^9 a_n f^n \tag{14}$$

where  $f$  represents the frequency in MHz.

Table III shows the building capacity (Mbps) distribution for different amount of transmit power [24].

It is interesting to note that for approximately 1 mW of transmit power, the average channel capacity for medium size buildings is close to 100 Mbps, 80% of channels have capacity in excess of 48 Mbps, and 99% of channels have capacity in excess of 14 Mbps. Such data rates are quite competitive with typical local area network rates based on dedicated wiring, and hence in some way confirm the potential commercial viability of power line communication.

### 5.2. RMS delay spread

The average RMS delay spread of a channel is a parameter that determines the frequency selectivity of the fading channel. Frequency selectivity in the time domain can be translated to

Table II. Test channel transfer function coefficients, where a channel transfer function is defined as:  $20 \log_{10}|H(f)| = \sum_{n=0}^9 a_n f^n$ , where  $f$  is frequency in MHz. (The transmit power is 1 mW.)

	$a_9$	$a_8$	$a_7$	$a_6$	$a_5$	$a_4$	$a_3$	$a_2$	$a_1$	$a_0$
TST1S	-3.439e-8	4.833e-6	-2.846	9.116e-3	-1.725e-1	1.967	-1.297	4.871e1	-8.718e1	2.314e1
TST2S	-1.074e-8	1.437e-6	-1.074e-8	2.400e-3	-4.231e-2	4.512e-1	-2.906	1.070e1	1.848e1	-2.195e1
TST3S	-3.257e-8	4.530e-6	-3.257e-8	8.218e-3	-1.511e-1	1.667	-1.094e1	4.099e1	7.949e1	1.465e1
TST4S	-7.925e-9	1.408e-6	-7.925e-9	1.670e-3	-2.875e-2	3.084e-1	-2.184	1.030e1	-2.687e1	-2.357e1
TST1M	2.119e-9	-1.906e-7	4.368e-6	9.207e-5	-6.298e-3	1.268e-1	-1.297	7.400	-2.246e1	-1.891e1
TST2M	-6.766e-9	5.695e-7	-9.893e-6	-4.914e-4	2.584e-2	-4.985e-1	4.772	-2.254e1	4.567e1	-5.945e1
TST3M	-4.069e-8	5.539e-6	-3.134e-4	9.555e-3	-1.704e-1	1.816	-1.144e1	4.141e1	-7.604e1	1.462e1
TST4M	2.362e-8	-3.338e-6	1.972e-6	-6.330e-3	1.200e-1	-1.367	9.125	-3.317e1	5.767e1	-8.124e1
TST1L	-1.567e-8	2.353e-6	-3.134e-4	5.132e-3	-1.055e-1	1.316	-9.763	4.006e1	-7.843e1	6.800
TST2L	-6.930e-8	9.619e-6	-5.566e-4	1.741e-2	-3.191e-1	3.489	-2.225e1	7.751e1	-1.271e2	2.32e1
TST3L	-2.861e-8	3.989e-6	-2.329e-4	7.388e-3	-1.386e-1	1.572	-1.066e1	4.141e1	-8.358e1	1.412e1
TST4L	-1.596e-8	2.118e-6	-1.150e-4	3.287e-3	5.290e-2	4.819e-1	-2.451	6.954	-1.015e1	-4.157e1

Table III. Test building capacity distribution (Mbps) for different transmit power levels.

Trans. Pow.	Type	99%	80%	50%	20%	1%	Type	99%	80%	50%	20%	1%
100 mW	Large 1	82	156	210	280	385	Large 2	38	111	175	247	383
10 mW	Large 1	30	95	142	196	292	Large 2	26	47	109	205	268
1 mW	Large 1	14	46	78	119	199	Large 2	9	15	57	129	183
100 $\mu$ W	Large 1	2	15	35	66	120	Large 2	2	5	25	68	104
10 $\mu$ W	Large 1	1	4	12	27	60	Large 2	0.8	1	7	28	49
1 $\mu$ W	Large 1	0.4	1.4	3	8	23	Large 2	0.3	0.4	1	9	17
100 mW	Medium 1	133	220	272	323	392	Medium 2	85	160	214	282	387
10 mW	Medium 1	69	142	187	231	304	Medium 2	32	99	143	198	295
1 mW	Medium 1	27	78	112	150	210	Medium 2	14	48	81	121	202
100 $\mu$ W	Medium 1	9	34	52	81	130	Medium 2	2	16	37	68	123
10 $\mu$ W	Medium 1	1	11	21	34	67	Medium 2	1	5	13	28	62
1 $\mu$ W	Medium 1	0.4	2	6	11	26	Medium 2	0.4	1.5	3	7	24
100 mW	Small 1	148	222	274	326	404	Small 2	103	180	231	291	393
10 mW	Small 1	80	154	191	234	308	Small 2	48	111	153	201	299
1 mW	Small 1	36	88	117	152	213	Small 2	21	62	93	130	207
100 $\mu$ W	Small 1	13	41	63	86	137	Small 2	6	27	47	72	127
10 $\mu$ W	Small 1	3	12	25	39	71	Small 2	1	7	19	32	65
1 $\mu$ W	Small 1	0.5	3	7	13	29	Small 2	0.5	2	5	10	26

time dispersion of the channel impulse response. In Reference [31] the author relates the RMS delay spread to the irreducible bit error probability in unequalized systems. If  $h(t)$  represents the impulse response of a channel and we define

$$p(t) = h^2(t) / \int_{-\infty}^{\infty} h^2(t) dt$$

then  $p(t)$  may be regarded as the probability density function for some random variable  $\tau$ . The RMS delay spread is then the standard deviation of  $\tau$  [32], i.e. the RMS delay spread can be computed as [32]

$$S_{\text{rms}} = (E[\tau^2] - E^2[\tau])^{1/2} \quad (15)$$

where expectations are computed with respect to the probability density function  $p$ .

The RMS delay spread for 10 000 channels in three different size buildings have been calculated and the cumulative distribution is shown in Figure 11. It is interesting to note that approximately 80% of all channels have an RMS delay spread less than 300 ns, and 99% have an RMS delay spread less than 500 ns.

## 6. CONCLUSION

The wide variety of possible wiring configurations in typical in-building power distribution networks presents the designer of a power line communication system with many interesting challenges.

In this work, we have developed a model that can be used to pseudorandomly generate an ensemble of realistic test channels for NEC-compliant power line circuits. Background noise and impulse noise, modelled on actual measurements, are included as part of the channel model.

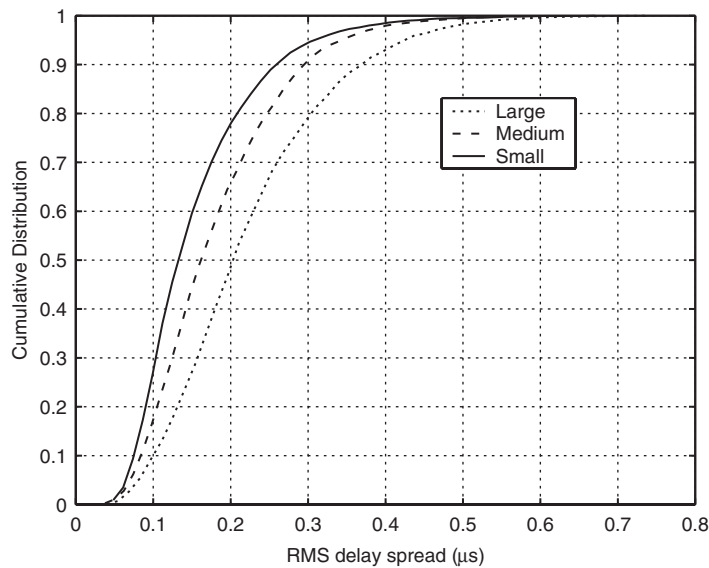


Figure 11. The cumulative distribution of RMS delay spread for different building size. (10000 random channels have been used in each curve).

Various parameters of each channel (e.g. channel capacity, RMS delay spread) are easily computed.

For example, capacity calculations for a large number of such channels drawn at random from the ensemble show that, even with a small transmit power limit of 1 mW, in the worst case of the 'Large 2' building type, 99% of all channels have a capacity greater than 9 Mbps, and 80% of all channels have a capacity greater than 15 Mbps. Typical channel capacities in other building types are even larger.

In some cases, it may be prohibitively expensive to test or simulate an actual modem with a large number of test channels. Thus a small number of test channel transfer functions have been chosen as being representative of different channel categories. These transfer functions can potentially serve as an unbiased set of cable plants to comparatively analyse power line modems.

We believe that the ensemble of channel models described in this work will be useful as a tool to guide communication system designers in developing power line modems that can adapt to a wide variety of channels, and hence achieve the large communication potential of in-building power lines.

#### REFERENCES

1. Hudson AG, Beuerle DR, Fiedler HJ. SSB carrier for utility control and communication. *Proceedings of the IEEE National Telecommunication Conference*, 1976; 2.1.1–2.1.7.
2. Lokken G, Jagoda N, D'Auteuil RJ. The proposed Wisconsin electric company load management system using power line over eistribution Lines. *Proceedings of the IEEE National Telecommunication Conference*, 1976; 2.2.1–2.2.3.
3. Van Der Gracht PK, Donaldson RW. Communication using pseudonoise modulation on electric power distribution circuits. *IEEE Transactions on Communication* 1985; COM-33:964–974.

4. Onunga JO, Donaldson RW. Personal computer communications on intrabuilding power line LAN's using CSMA with priority acknowledgments. *IEEE Journal on Selected Areas in Communication* 1989; 7:180–191.
5. Vuong ST, Ma AHT. A low-cost and portable local area network for interconnecting PC's using electric power lines. *IEEE Journal on Selected Areas in Communication* 1989; 7:192–201.
6. Dostert KM. Frequency-hopping spread-spectrum modulation for digital communications over electrical power lines. *IEEE Journal on Selected Areas in Communication* 1990; 8:700–710.
7. Karl M, Dostert KM. Selection of an optimal modulation scheme for digital communications over low voltage power lines. *Proceedings of the IEEE International Symposium on Spread Spectrum*, Mainz, Germany, September 1996; 1087–1091.
8. Ozawa Y, Arai T, Kohno R. Spread spectrum transmission systems using the earth returning circuit on a low-voltage distribution line. *Proceedings of the IEEE International Symposium on Spread Spectrum*, Mainz, Germany, September 1996; 1097–1101.
9. Marubayashi G, Tachikawa S. Spread spectrum transmission on residential power line. *Proceedings of the IEEE International Symposium on Spread Spectrum*, Mainz, Germany, September 1996; 1082–1086.
10. Rice BF. A multiple-sequence spread spectrum system for powerline communications. *Proceedings of the IEEE International Symposium on Spread Spectrum*, Mainz, Germany, September 1996; 809–815.
11. Esmailian T, Gulak, PG, Kschischang FR. A discrete multitone power line communications system. *Proceedings of ICASSP'2000* 2000; 5:2953–2956.
12. Han Vinck AJ, Lindell G. Summary of Contributions at ISPLC 1997–2001. *Proceedings of the 5th International Symposium on Power-Line Communications and Applications*, 2001; 383–413.
13. Palmquist RE. *Guide to the 1990 National Electrical Code*. MacMillan: New York, 1990.
14. Chan MHL. Channel characterization and forward error correction coding for data communications on intrabuilding electric power lines. *Ph.D. Thesis*, The University of British Columbia, Department of Electrical Engineering, 1988.
15. Hooijen O. *Aspects of Residential Power Line Communications*. Shaker Verlag: Aachen, 1998.
16. Gardner S. The homeplug standard for powerline home networking. *Proceedings of the 5th International Symposium on Power-Line Communications and Applications*, 2001; 67–72.
17. Tsuzuki S, Yamamoto S, Takamatsu T, Yamada Y. Measurement of Japanese indoor power-line channel. *Proceedings of the 2000 International Symposium on Power-line Communications and Application*, Limerick, Ireland, April 2000; 79–84.
18. Cogency Semiconductor Inc., *Powerline-based Networking*, available online at: [http://www.cogency.com/B.htm/PBL3\\_B6.Powerline.htm](http://www.cogency.com/B.htm/PBL3_B6.Powerline.htm).
19. McPartland JF, McPartland BJ. *Handbook of Practical Electrical Design* (3rd edn). McGraw-Hill: New York, 1999.
20. Traister JE. *Illustrated Guide to the National Electrical Code*. Craftsman Book Company: Carlsbad, CA 1993.
21. Temes GC, Lapatra, JW. *Introduction to Circuit Synthesis and Design*. McGraw-Hill: New York, 1967.
22. Irwin JD. *Basic Engineering Circuit Analysis*. MacMillan: New York, 1987.
23. Werner JJ. The HDSL Environment. *IEEE Journal on Selected Areas in Communications* 1991; 9:785–800.
24. Esmailian T. Multi mega-bit per second data transmission over in-building power lines. *Ph.D. Thesis*, Department of Electrical and Computer Engineering, University of Toronto, 2002.
25. Esmailian T, Kschischang FR, Gulak PG. Characteristics of in-building power lines at high frequencies and their channel capacity. *Proceedings of the 2000 International Symposium on Power-line Communications and Applications*, Limerick, Ireland, April 2000; 52–59.
26. Philipps H. Performance measurement of powerline channels at high frequencies. *Proceedings of the 1998 International Symposium on Power-line Communications and Applications*, Tokyo, Japan, March 1998; 229–237.
27. Press WH, Flannery BP, Teukolsky SA, Vetterling WT. *Numerical Recipes in C*. Cambridge University Press, Cambridge, MA, 1998.
28. Chan MHL, Donaldson RW. Amplitude, width, and interarrival distributions for noise impulses on intrabuilding power line communication networks. *IEEE Transactions on Electromagnetic Compatibility* 1989; 31:320–323.
29. *The Student Edition of MATLAB: version 5, user's guide*/The Mathworks Inc., Prentice-Hall, Upper Saddle River, NJ, 1997.
30. Gallager RG. *Information Theory and Reliable Communication*. Wiley: New York, 1968.
31. Bello P. Characterization of randomly time-variant linear channels. *IEEE Transactions on Communications* 1963; 11:360–393.
32. Molisch AF. *Wideband Wireless Digital Communications*. Prentice-Hall: Upper Saddle River, NJ, 2001.

## AUTHORS' BIOGRAPHIES



**Tooraj Esmailian** received the BSc degree from Isfahan University of Technology, Isfahan, Iran, in 1992, the MSc degree from Sharif University of Technology, Tehran, Iran, in 1995, and the PhD degree from the University of Toronto, Toronto, Canada in 2003, all in electrical engineering. While at the University of Toronto, he was supported by a grant from Motorola, and received an international student award from the University of Toronto in 1998, a University of Toronto open fellowship in 1999, and Ontario graduate scholarships in 2000 and 2001.

He is now with the research and development group of Cogency Semiconductor Inc., Kanata, Ontario, Canada, working on HomePlug-based power line products. His research interests are in the general area of digital communications, especially multicarrier modulation, error control coding, and channel modelling.



**Frank R. Kschischang** received an honours BSc degree from the University of British Columbia in 1985, and MASc and PhD degrees from the University of Toronto in 1988 and 1991, respectively, all in electrical engineering. Since 1991 he has been a faculty member in the Department of Electrical and Computer Engineering at the University of Toronto, where he holds the rank of Professor and the title Canada Research Chair in Communication Algorithms. His research interests are focussed on the area of coding techniques, primarily on efficient and effective iterative decoding algorithms and their applications. He is the recipient of an Ontario Premier's Research Excellence Award.



**P. Glenn Gulak** received the PhD degree from the University of Manitoba, Winnipeg, MB, Canada. From 1985 to 1988, he was a Research Associate with the Information Systems Laboratory and the Computer Systems Laboratory, Stanford University, Stanford, CA. Currently he is a Professor with the Department of Electrical and Computer Engineering, at the University of Toronto, Toronto, ON, Canada, and holds the L. Lau Chair in Electrical and Computer Engineering. His research interests are in the areas of memory design, circuits, algorithms, and VLSI architectures for digital communications.

Dr Gulak received a Natural Sciences and Engineering Research Council of Canada Postgraduate Scholarship and several teaching awards for undergraduate courses taught in both Department of Computer Science and Department of Electrical and Computer Engineering of the University of Toronto, Toronto, ON, Canada. He has served on the ISSCC Signal Processing Technical Subcommittee since 1990 and served as the Technical Program Chair for ISSCC 2001. He is a registered professional engineer in the province of Ontario.